doi:10.1016/j.ijrobp.2005.01.045

L-(METHYL-11C) METHIONINE POSITRON EMISSION TOMOGRAPHY FOR TARGET DELINEATION IN RESECTED HIGH-GRADE GLIOMAS BEFORE RADIOTHERAPY

Anca-Ligia Grosu, M.D.,* Wolfgang A. Weber, M.D.,† Eva Riedel, M.D.,*
Branislav Jeremic, M.D.,* Carsten Nieder, M.D.,* Martina Franz,*
Hartmut Gumprecht, M.D., Ruprecht Jaeger, M.D.,§ Markus Schwaiger, M.D.,†
and Michael Molls, M.D.*

Departments of *Radiation Oncology, and §Neurosurgery, Klinikum Rechts der Isar, Technical University of Munich,
Munich, Germany; †Department of Nuclear Medicine, Krankenhaus München-Bogenhausen,
Munich, Germany

Purpose: Using magnetic resonance imaging (MRI), residual tumor cannot be differentiated from nonspecific postoperative changes in operated patients with brain gliomas. The higher specificity and sensitivity of L-(methyl-11C)-labeled methionine positron emissions tomography (MET-PET) in gliomas has been demonstrated in previous studies and is the rationale for the integration of this investigation in gross tumor volume delineation. The goal of this trial was to quantify the affect of MET-PET vs. with MRI in gross tumor volume definition for radiotherapy planning of high-grade gliomas.
Methods and Materials: The trial included 39 patients with resected malignant gliomas. MRI and MET-PET data were coregistered based on mutual information. The residual tumor volume on MET-PET and the volume of tissue abnormalities on T_1-weighted MRI (gadolinium [Gd] enhancement) and T_2-weighted MRI (hyperintensity areas) were compared using MET-PET/MRI fusion images.
Results: The MET-PET vs. Gd-enhanced T_1-weighted MRI analysis was performed on 39 patients. In 5 patients (13%), MET uptake corresponded exactly with Gd enhancement, and in 29 (74%) of 39 patients, the region of MET uptake was larger than that of the Gd enhancement. In 27 (69%) of the 39 patients, the Gd enhancement area extended beyond the MET enhancement. MET uptake was detected up to 45 mm beyond the Gd enhancement. MET-PET vs. T_2-weighted MRI was investigated in 18 patients. MET uptake did not correspond exactly with the hyperintensity areas on T_2-weighted MRI in any patient. In 9 (50%) of 18 patients, MET uptake extended beyond the hyperintensity area on the T_2-weighted MRI, and in 18 (100%), at least some hyperintensity on the T_2-weighted MRI was located outside the MET enhancement area. MET uptake was detected up to 40 mm beyond the hyperintensity area on T_2-weighted MRI.
Conclusion: In operated patients with brain gliomas, the size and location of residual MET uptake differs considerably from abnormalities found on postoperative MRI. Because postoperative changes cannot be differentiated from residual tumor by MRI, MET-PET, with a greater specificity for tumor tissue, can help to outline the gross tumor volume with greater accuracy. © 2005 Elsevier Inc.

High-grade gliomas, Radiotherapy, Biologic target volume, Methionine positron emission tomography, MRI.

INTRODUCTION

The standard tools in the diagnosis and treatment planning of malignant gliomas (1–12) are magnetic resonance imaging (MRI) and computed tomography (CT) (13–15). Tumor tissue can be visualized on MRI and CT because of the increased water content (edema) compared with normal brain tissue and because of the blood–brain barrier (BBB) disruption, visualized as contrast enhancement. However, neither contrast enhancement nor edema is always a real measure of tumor extension in low- and high-grade gliomas. Tumor cells have been detected beyond the margins of contrast enhancement, in the surrounding edema, and even in the adjacent normal-appearing brain tissue. After neurosurgery or radiotherapy (RT), BBB disturbances and edema can also be treatment-related and cannot be differentiated from persistent tumor on CT or MRI (16–18). These issues

---

clearly call for new methods of defining the tumor volume more precisely.

Recently, new methods of tumor visualization have conquered the domain of radiation oncology. Techniques such as positron emission tomography (PET), single photon emission CT (SPECT), and magnetic resonance spectroscopy (MRS) are able to visualize the biologic pathways of tumors, giving additional information about the metabolism, physiology, and molecular biology of the tumor tissue (19–21). A new class of images, showing a specific biologic event, has the potential to complement the anatomic information of traditional radiologic techniques. This new class of images is called biologic images. Thus, in addition to the concepts of the gross, clinical, and planning target volume (GTV, CTV, and PTV, respectively), Ling *et al.* (19) proposed using the concepts of the biologic target volume and multidimensional conformal RT.

This study analyzed the affect of a biologic image investigation, L-(methyl-11C)-labeled methionine-PET (MET-PET) for the visualization of tumor extension in brain gliomas.

L-(methyl-11C)-labeled methionine is a natural amino acid avidly taken up by glioma cells, with only a low uptake in normal cerebral tissue. The uptake is mainly mediated by the L-type amino acid transport system. MET may be used for protein synthesis or converted to S-adenosylmethionine, which is the primary methyl donor for transmethylation reactions and a precursor of polyamide synthesis. A smaller part of MET is metabolized by decarboxylation. However, several experiments have suggested that during PET studies, tumor uptake of MET mainly reflects increased amino acid transport (22–24). A comparative analysis between CT, MRI, and MET-PET and stereotactic biopsies suggested that MET-PET has greater accuracy in defining the extent of gliomas than CT and MRI (25–28). Herholz *et al.* (29) showed the sensitivity and specificity of MET-PET in differentiating between nontumoral tissue and low-grade gliomas to be 76% and 87%, respectively.

No data in the literature have quantified the tumor extension in MET-PET and MRI and compared these two imaging modalities using image fusion. In the era of the integrated PET-CT scanner, this analysis is of high importance. We undertook the present study to quantify the affect of MET-PET compared with MRI for the delineation of tumor extension of high-grade gliomas and to show its implication for treatment planning. Therefore, the extension of gadolinium (Gd) enhancement on T_1-weighted MRI and the hyperintensity area on T_2-weighted MRI were compared with the extension of MET uptake on PET, using MET-PET/MRI fusion.

METHODS AND MATERIALS

Patients

The study included 39 patients with high-grade gliomas who had undergone tumor resection. The inclusion criteria for the trial were the diagnosis (or suspicion) of residual tumor on MRI performed 24 hours postoperatively and/or the intraoperative diagnosis of possible residual tumor. The 20 men and 19 women had a median patient age of 53 and 55 years, respectively (range 26–78) and a Karnofsky performance status between 60% and 100%.

Of the 39 patients, 27 had glioblastoma, 9 anaplastic astrocytoma, and 3 anaplastic oligodendroglioma. CT, MRI, and MET-PET for treatment planning were all performed in the same week, 1–4 weeks after surgical tumor resection. The steroid dose was not changed in the week in which the MRI and PET examinations were performed. The institutional ethics committee approved the study protocol, and all patients provided written informed consent.

MRI

MRI for treatment planning was performed using a Philips 1.5 Tesla scanner Gyroscan ACS-NT. The head was not fixed during MRI. The acquisition was done with a standard head coil. Axial T_1-weighted native and after contrast administration (Gd-diethylenetriaminepentaacetic acid [Gd-DTPA], 0.1 mmol/kg body weight) and T_2-weighted images were acquired from the foramen magnum to the vertex, orthogonal to the holder plate of the mask. The slice thickness was 1.5 mm, without gaps. The MRI data were transferred via network to the BrainLAB stereotactic treatment planning system (BrainLAB, Heimstemen, Germany).

MET-PET

Patients fasted for at least 4 hours before MET-PET to ensure standardized metabolic conditions. The PET studies were acquired using an ECAT EXACT HR+ PET scanner (CT1/Siemens; Siemens Medical Systems, Concord, CA). This imaging device consists of 62 detectors that yield 63 transverse slices 2.4 mm apart (axial field of view 15 cm). According to NEMA standards, the spatial resolution in the axial and transaxial directions is 5 mm. Before MET injection, a transmission scan of 5-min duration (approximately 1.5 million counts/slice) was acquired (30). Emission data corrected for attenuation, scatter, and random coincidences were reconstructed by filtered back projection using a Hanning filter with a cutoff frequency of 0.5 cycles/bin. Carrier-free MET (specific activity >18.5 GBq/μmol) was synthesized from (11C)methyl iodide and homocysteine (31). A static emission scan of 15-min duration was acquired in two-dimensional mode 15 min after injection of 300–370 MBq MET. After the MET-PET procedure, the data were transferred via network to the BrainLAB stereotactic treatment planning system.

CT

Computed tomography was performed with a Siemens Somatom AR HP. The head was immobilized in a commercially available stereotactic mask (BrainLAB). Before the investigation began, a contrast medium (Ioversol, Optiray 300) was administered intravenously. The data were transferred via network to the BrainLAB stereotactic treatment planning system.

PET/MRI/CT image fusion

The images were analyzed using the MET-PET/CT/MRI BrainLAB fusion software. The validation of this fusion system was already published (32). The automatic image fusion software (BrainLAB) is based on the mutual information measure and does not require any user interaction, thus eliminating interobserver variability in the image fusion process. The computing time for the automatic image fusion on a standard workstation (Pentium II, 450 MHz) is less than 2 min. The algorithm's robustness was evalu-

ated, and the discrepancy of fusion results due to the different initial image alignments was determined to be <1 mm inside the test volume of interest.

Determination of residual tumor volume in MET-PET/ MRI fusion images and volume of tissue abnormalities in T_1- and T_2-weighted MRI

The MET-PET and MRI studies were analyzed by two independent observers with neuroradiology and nuclear medicine training (A.L.G. and W.A.W.). The MET-PET, MRI, and MET-PET/MRI images were analyzed separately in each patient.

The residual tumor volume defined by focal MET uptake in the MET-PET and MET-PET/MRI images (Vol-MET) was delineated manually. However, a threshold value for the tumor/normal tissue index of 1.7 was considered for the tumor margin in all patients. This value was determined in a study that analyzed the sensitivity and specificity of MET-PET in malignant brain tumors (manuscript in preparation). For all the patients included in the trial, the same windowing was used. An automated definition of tumor volume was not feasible because of the small size of focal MET uptake in most patients and the high uptake in normal tissue such as lacrimal glands or mucosa. All MRI voxels included in the delineated area were calculated in the Vol-MET.

The investigators delineated the hyperintensity signal in the T_2-weighted images showing tumor tissue, edema, and postoperative changes, inclusive of the resection cavity (Vol-T_2) and the contrast-enhancement areas in the T_1-weighted images, corresponding to tumor tissue or BBB disturbances postoperatively (Fig. 1). The blood areas were subtracted using the comparative analysis of the native T_1 studies. The volume of the pathologic brain tissue changes on MRI was calculated by multiplying the slice thickness by the encompassed surface.

Statistical analysis

The statistical analysis included the automatic quantification of the following pathologic changes on PET and MRI (Fig. 1):

1. The evaluation of pathologic MET uptake volume, as delineated on the MET-PET and MET-PET/MRI fusion images (Vol-MET).
2. The evaluation of the hyperintensity area in the T_2-weighted images (Vol-T_2) and evaluation of the Gd-DTPA enhancement volume on the T_1-weighted images (Vol-Gd).
3. For those with MET uptake located outside the changes on MRI, the composite volume MRI/PET (composite Vol-Gd/ MET and composite Vol-T_2/MET) were calculated, using the results of the fusion images: composite Vol-Gd/MET = Vol-Gd ∪ Vol-MET and composite Vol-T_2/MET = Vol-T_2 ∪ Vol-MET, where ∪ indicates union.
4. The volume of MET uptake on PET and the pathologic changes on MRI were computed together under common volume MRI/PET (common Vol-Gd/MET and common Vol-T_2/ MRI): common Vol-Gd/MET = Vol-Gd ∩ Vol-MET and common Vol-T_2/MET = Vol-T_2 ∩ Vol-MET, where ∩ indicates intersection.
5. In patients with MET uptake located outside the changes on MRI, we calculated the volume of MET uptake located outside the changes on MRI (Vol MET minus MRI): Vol-(MET minus Gd) and Vol-(MET minus T_2). In each patient (as determined by the MRI/PET fusion), the maximal distance between the margin of the MRI changes and the margin of the MET uptake (in millimeters) was quantified.
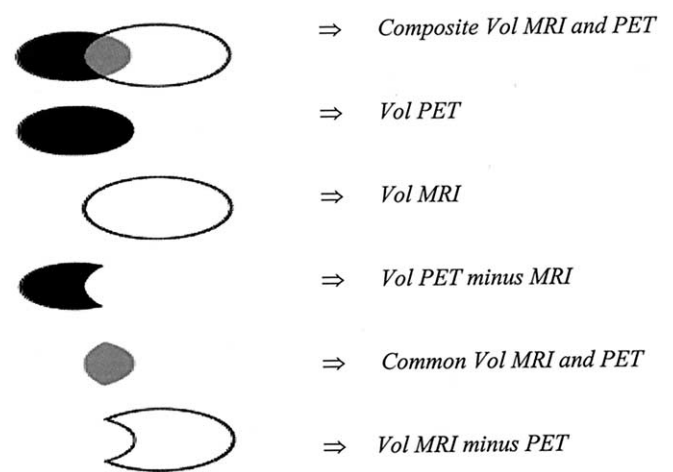

Fig. 1. Presentation of volumes quantified on MRI/PET fusion images. MRI = magnetic resonance imaging; PET = positron emission tomography.

6. The volume of the pathologic changes in MRI located outside of the region with MET tumor uptake was computed as Vol-(Gd minus MET) and Vol-(T_2 minus MET).

Vol-MET, Vol-T_1, and Vol-T_2 were calculated after the manual delineation. The other volumes were computed automatically.

All statistical analyses were performed using the Statistical Package for the Social Sciences for Windows software (SAS Institute, Cary NC).

RESULTS

A total of 39 patients with malignant glioma were entered into this study. T_1-weighted MRI with Gd and MET-PET scans were analyzed for all 39 patients, and T_2-weighted MRI scans were quantified for only 18 patients. MET uptake indicating residual tumor was detected in all 39 patients. Gd enhancement was found on T_1-weighted MRI in all 39 patients and hyperintensity areas on T_2-weighted MRI were outlined in all 18 cases. The results of the volumetric measurements for all patients are given in Tables 1 and 2.

MET-PET vs. T_1-weighted MRI with Gd

The results of volumetric measurements on MET-PET, T_1-weighted MRI with Gd and MET-PET/MRI fusion in 39 patients with malignant gliomas are presented in Tables 1, 3, and 4 and Figs. 2–5 (see also Fig. 7).

For the whole group, the mean Vol-Gd was 11 cm³ (range, 1–69). The mean Vol-MET was 19 cm³ (range, 1–102 cm³). The mean composite Vol-(Gd ∪ MET) was 24 cm³, and the mean common Vol-(Gd ∩ MET) was 6 cm³. The mean Vol-(Gd minus MET) was 6 cm³ (range, 0–60 cm³), and the mean Vol-(MET minus Gd) was 13 cm³ (range, 0–101 cm³). MET uptake was detected up to 45 mm beyond Gd enhancement (range, 1–45). In 11 (28%) of 39 patients, MET uptake extended >25 mm from the margin of Gd enhancement (Tables 1 and 3).

Finally, on the basis of the PET/MRI fusion images, areas

Table 1. Results of volumetric measurements of T_1-weighted MRI vs. MET-PET in 39 patients with resected malignant gliomas

Pt. No.	Vol-MET (cm³)	Vol-Gd (cm³)	Composite Vol-Gd/MET (cm³)	Common Vol-Gd/MET (cm³)	Vol-(Gd minus MET) (cm³)	Vol-(MET-minus-Gd) (cm³)
1	4.9	7.6	7.6	4.9	2.7	0
2	19.1	2.6	19.1	2.6	0	16.5
3	27.3	27.3	27.3	27.3	0	0
4	2.6	2.1	4.7	0.1	2.1	2.5
5	0	7.06	0	7.06	7.06	0
6	0	0.79	0	0.79	0.79	0
7	38.8	3.9	38.8	3.9	0	34.9
8	9.2	8.8	15.9	2.2	6.7	7
9	22.1	27.5	37.4	12.3	15.3	9.8
10	30	30	30	30	0	0
11	0	4.71	0	4.71	4.71	0
12	1.9	5	6.3	0.6	4.4	1.3
13	57.6	53.2	92	18.8	34.4	38.8
14	4.6	13.7	15.4	2.7	10.9	1.8
15	19.6	13.5	21.8	11.2	2.2	8.4
16	7.2	7	11.4	2.8	4.2	4.4
17	13.3	69.1	73	9.5	59.7	3.8
18	17.7	10.2	19.4	8.3	1.8	9.3
19	19	34	46.9	6.1	27.9	12.9
20	8	8	8	8	0	0
21	9.1	9.9	15.8	3.2	6.7	5.9
22	1.7	1.7	1.7	1.7	0	0
23	78.4	5.1	78.4	4.9	0	73.5
24	25	2.5	26.2	1.3	1.2	23.7
25	20.2	15.9	33.2	2.9	13	17.3
26	5.5	2.7	6.9	1.3	1.4	4.2
27	38.3	1.7	38.3	1.7	0	36.6
28	1.9	1.9	3.2	0.6	1.3	1.3
29	17.8	3.3	18.8	2.3	1	15.5
30	4.9	6.1	6.6	4.9	1.7	0
31	2.6	0.6	2.8	0.4	0.2	2.2
32	29.9	5.6	30.1	5.5	0.2	24.4
33	13.3	9.3	15.6	7.1	2.3	6.2
34	27.4	0.7	27.4	0.7	0	26.7
35	5	0.6	5.6	0	0.6	5
36	12	12	12	12	0	0
37	17.2	12.3	20.6	8.9	3.4	8.3
38	101.5	1.1	101.6	1.1	0	100.5
39	9.1	2.3	9.2	2.3	0	6.9

See text for description of terms used.

with MET uptake on PET were compared with the Gd-enhanced regions on T_1-weighted MRI (Table 4). MET uptake and Gd enhancement were detected in all 39 patients. In 5 patients (13%) MET uptake corresponded exactly with the Gd enhancement, and in 29 patients (74%) MET uptake was also located outside the Gd enhancement. In 27 patients (69%), Gd enhancement was also located outside the MET enhancement.

MET-PET vs. T_2-weighted MRI

The results of the volumetric measurements in 18 patients with resected malignant gliomas, in whom T_2-weighted MRI was compared with MET-PET, are given in Tables 2, 5, and 6 and Figs. 2–4 and Fig. 6.

For all 18 analyzed cases, the mean Vol-T_2 was 42 cm³ (range, 3–150 cm³). The mean Vol-MET was 23 cm³ (range, 2–102 cm³). The mean composite Vol-($T_2 \cup$ MET) was 52 cm³, and the mean common Vol-($T_2 \cap$ MET) was 13 cm³. The mean Vol-(T_2 minus MET) was 29 cm³ (range, 1–138 cm³), and the mean Vol-(MET minus T_2) was 10 cm³ (range, 0–78 cm³). MET uptake was identified up to 40 mm (range 1–40) beyond the hyperintensity areas on T_2-weighted MRI. In 7 (39%) of 18 patients, MET uptake extended >25 mm from the margin of Gd enhancement.

Finally, on the basis of PET/MRI fusion images, the areas with MET uptake on PET were compared with the hyperintensity areas on T_2-weighted MRI (Table 6). MET uptake and hyperintensity area on T_2-weighted MRI were observed in all investigated cases. The extension of MET uptake was different from the hyperintensity areas. Some MET uptake was located outside the hyperintensity area, as well as inside (9 of 18 patients, 50%), but in 100%, the hyperintensity

Table 2. Results of volumetric measurements of T_2-weighted MRI vs. MET-PET in 18 patients with resected malignant gliomas

Pt. No.	Vol-MET (cm^3)	Vol-T_2 (cm^3)	Composite Vol-(T_2 and MET) (cm^3)	Common Vol-(T_2 and MET) (cm^3)	Vol-(T_2 minus MET) (cm^3)	Vol-(MET minus T_2) (cm^3)
1	1.7	19.6	19.6	1.7	17.9	0
2	78.4	133.6	133.6	78.4	55.2	0
3	25	14.5	31.8	7.8	6.8	17.2
4	20.2	35.9	49.2	6.8	29	13.4
5	5.5	21.1	21.1	5.5	15.6	0
6	38.3	46.3	57.6	27	19.3	11.3
7	1.9	18.5	18.5	1.9	16.6	0
8	17.8	14.5	26.4	5.9	8.6	11.9
9	4.9	5.3	5.9	4.9	1	0
10	2.6	7.7	9	2.6	6.4	0
11	29.9	34.5	50.7	13.8	20.7	16.2
12	13.3	95.3	95.3	13.3	82	0
13	27.4	17.9	44.4	0.8	17	26.6
14	5	4.6	9.3	0.3	4.3	4.7
15	12	150	150	12	138	0
16	17.2	77.3	77.3	17.2	60.1	0
17	101.5	51	128.5	24	27	77.5
18	9.1	3.1	10.1	2.1	1	7

See text for description of terms used.

region on T_2-weighted MRI extended beyond the MET enhancement area.

DISCUSSION

MET-PET, IMT-SPECT, and 0-(2-[18F]Fluoroethyl)-L-tyrosine (FET)-PET in tumor volume definition of gliomas

The results of this study have demonstrated the high impact of MET-PET in the visualization of tumor extension for operated patients with high-grade brain gliomas. The volume of MET uptake corresponded to the volume of Gd enhancement in only 13% of investigated patients and to the volume of hyperintensity areas on T_2-weighted MRI in no patient. In most patients, differences in both directions were observed: either a pathologic signal on PET without correlation on MRI or vice versa (Fig. 7).

MET uptake was located beyond Gd enhancement on MRI in 74% of cases and was identified outside the hyperintensity areas on T_2-weighted MRI in 50% of patients. These findings have significant implications in the treatment strategy for patients with high-grade gliomas. They could help to plan not only RT, but also surgery and the local application of gene therapy, immunotherapy, or chemotherapy. The correct evaluation of the results of surgery also has significant implications in determining the prognosis, including both survival time and quality of life (33–35). In addition, the indication of other treatment strategies, such as RT and chemotherapy, are affected by the proper evaluation of the surgical results.

Concerning the planning of RT, the additional information from MET-PET can help to define the GTV, CTV, and PTV with high accuracy, something impossible to obtain 1–8 weeks after surgery using MRI alone. We showed that MET uptake was located up to 45 mm beyond Gd enhancement on MRI in 74% of cases and was identified up to 40 mm outside the hyperintensity areas on T_2-weighted MRI in 50% of patients. In a significant number of cases (i.e., 11 [28%] of 39 patients), MET uptake was located >25 mm from the margin of Gd enhancement and in 7 (39%) of 18 patients, >25 mm from the margin of T_2. The MET uptake

Table 3. Results of volumetric measurements in 39 patients with completely or partially resected brain gliomas

Volume (cm^3)	Gd	MET	Composite Gd and MET	Common Gd and MET	Gd-MET (minus)	MET-Gd (minus)
Mean	11	19	24	6	6	13
Median	6	13	16	3	2	7
SD	15	21	25	7	12	21
Minimum	1	0	0	0	0	0
Maximum	69	102	102	30	60	101

MRI and MET-PET performed 1–4 weeks postoperatively; volumetric measurements performed on PET/MRI fusion images; following volumes quantified: volume of Gd enhancement on T_1-weighted MRI, volume of MET uptake on PET, composite volume (Gd ∪ MET), common volume (Gd ∩ MET), volume of Gd enhancement without (minus) MET uptake, and volume of MET uptake without (minus) corresponding Gd enhancement.

Table 4. Results of comparison of Gd and MET in 39 patients using PET/MRI fusion images

Finding	*n* (%)
MET uptake corresponded to Gd enhancement	5/39 (13)
MET uptake located outside Gd enhancement	29/39 (74)
Gd enhancement located outside MET uptake	27/39 (69)

Areas with MET uptake on PET were compared, scan by scan, with areas with Gd enhancement on T_1-weighted MRI.

located outside of the MRI changes was not uniformly distributed around the margins of the radiologic abnormalities (Figs. 2–4). Therefore, it would not be possible to indicate a uniform margin around the MRI changes to ensure that the tumor tissue would be completely encompassed in the radiation field. Thus, MET-PET images have an essential role in the visualization of macroscopic tumor extension (GTV) and consequently will influence the CTV and PTV delineation. Microscopic tumor infiltration (CTV) should be defined with a margin of about 20 mm to the GTV and to the resection cavity.

An important consequence of the integration of MET-PET in the tumor volume delineation for gliomas is better sparing of the normal brain tissue. Gd enhancement and edema extended outside the MET uptake in 69% and 100% of cases, respectively. The mean volume of the Gd enhancement located outside of MET uptake was 6 cm^3, and the mean volume of the hyperintensity area on T_2 that extended beyond the MET uptake was 29 cm^3 (Table 5). Considering that Gd enhancement and edema that are located beyond the MET uptake were a result of the surgery, these regions should be excluded from the GTV and, as a consequence, would not be incorporated in the high radiation dose areas. Consequently, MET-PET will be useful for excluding normal brain tissue from the high radiation dose.
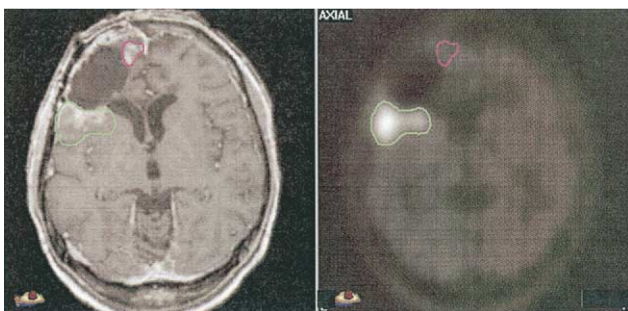

Fig. 3. Glioblastoma Grade IV, 4 weeks postoperatively and 3 days before radiotherapy. (a) T_1-MRI with Gd enhancement. Magnetic resonance imaging (MRI) and positron emission tomography (PET) data were coregistered using BrainLAB fusion software. Area with Gd enhancement on MRI outlined in pink and includes both residual tumor and BBB disturbances postoperatively. Area with L-methyl-11C)-labeled methionine (MET) uptake on MET-PET (green) indicates residual tumor tissue (gross tumor volume). MET uptake also extended outside Gd-enhancement area (yellow arrow), and Gd enhancement extended outside of MET uptake (blue arrow).

In previous studies, we investigated the impact of ^{123}I-labeled α-methyl-tyrosine-single photon computed emission tomography (IMT-SPECT) on the GTV definition for three-dimensional treatment planning of brain gliomas. IMT is an amino acid tracer with similar properties to MET for the visualization of gliomas (36, 37). Using MRI/SPECT fusion images, the GTV from SPECT was compared with the volume of hyperintensity regions on T_2-weighted MRI and with the volume of Gd enhancement on T_1-weighted MRI.

Initially, we investigated 30 nonoperated low- and high-grade glioma patients (38). In most cases, the hyperintensity

Fig. 2. Astrocytoma World Health Organization Grade III, 2 weeks postoperatively and 4 days before RT. (a) T_1-MRI scan with Gd enhancement. (b) MET-PET image. MRI and PET data were coregistered using BrainLAB fusion software. Area with both Gd and MET enhancement located in right temporal lobe (outlined in green) corresponds to residual tumor tissue and represents GTV. Small Gd enhancement area located in right temporal lobe (pink) shows no MET uptake on PET, indicating BBB disturbance from surgery and not included in GTV. MRI = magnetic resonance imaging; RT = radiotherapy; PET = positron emission tomography; GTV = gross tumor volume.
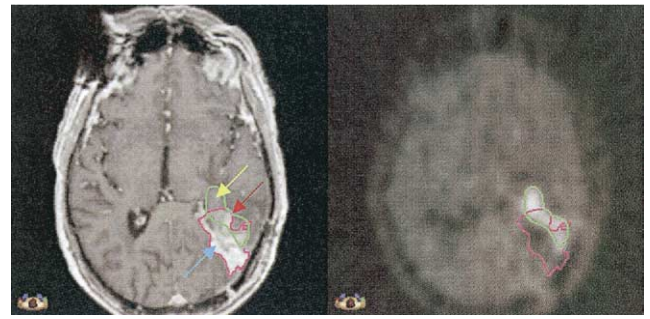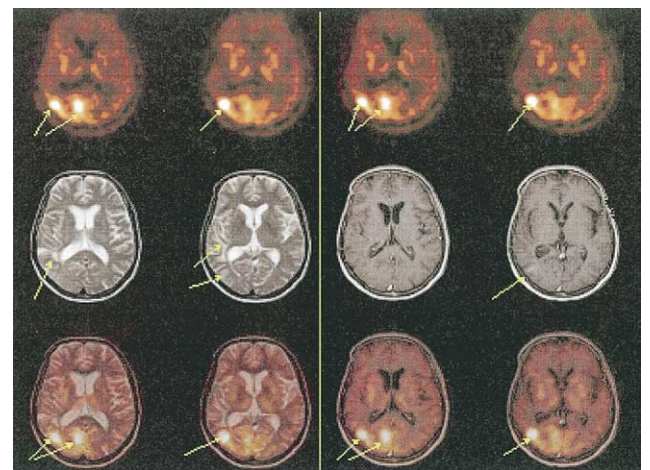

Fig. 4. Glioblastoma. L-(methyl-11C)-labeled methionine-positron emission tomography (MET-PET), T_2-weighted magnetic resonance imaging (MRI), T_1-weighted MRI with Gd, and PET/MRI fusion images. Yellow arrows indicate hyperintensity areas on T_2-weighted MRI, Gd enhancement on T_1-weighted MRI, and pathologic MET uptake on PET. Note, intensive MET uptake outside of changes seen on MRI.
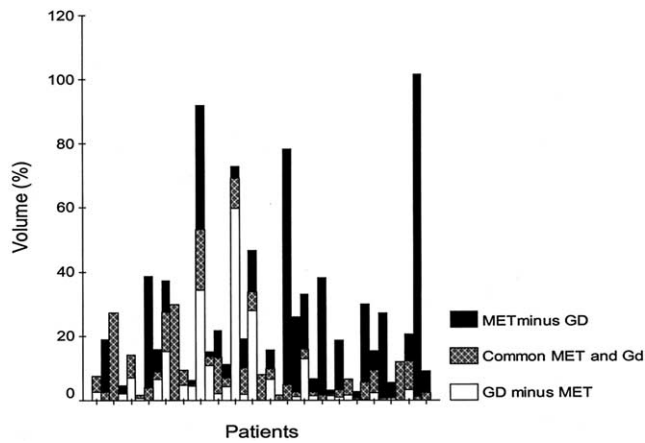
Fig. 5. T_1-weighted magnetic resonance imaging (MRI) with Gd vs. L-(methyl-11C)-labeled methionine-positron emission tomography (MET-PET). Volumetric measurements using PET/MRI fusion for 39 patients with resected gliomas. White bars indicate Gd outside of MET uptake; gray bars, both Gd and MET uptake; and black bars, MET uptake without Gd enhancement.

Fig. 7. Summary of our results. White circle represents mean volume of Gd enhancement without correlation with L-(methyl-11C) labeled-methionine (MET) uptake, indicating high probability of BBB disturbances postoperatively. Gray circle represents mean volume of tissue with both Gd enhancement and MET uptake. Black circle represents mean volume with MET uptake located outside of Gd enhancement on magnetic resonance imaging. Both gray and black areas should be considered macroscopic tumor tissue and included in gross tumor volume.

area on T_2-weighted MRI included the area with IMT-increased uptake on SPECT, confirming that T_2-changes incorporate both tumor tissue and perifocal edema. However, the most striking finding of the study was the observation that the IMT tumor uptake also extended up to 20 mm outside the T_2-weighted MRI changes in 23% of patients (7 of 30, all high-grade gliomas). By adding the additional IMT-SPECT information to the T_2-weighted MRI, a mean relative increase of the GTV of 33% was obtained. Comparing the IMT uptake with the Gd-enhancement areas on the T_1-weighted MRI/SPECT fusion images,

we observed that the IMT tumor uptake incorporated the contrast enhancement regions in all cases, and also extended outside the Gd-enhancing regions. In conclusion, that study showed that IMT-SPECT provided significant information regarding the extent of tumor tissue.

Consequently, we analyzed the affect of IMT-SPECT for GTV delineation in 66 patients with low- and high-grade gliomas after surgical resection (39). The design and results of that trial are comparative to those of the present study (Table 7). Analogous to the data presented in this study for MET, we found that the size and location of IMT uptake were not related to the abnormalities on postoperative T_1-weighted Gd-enhanced MRI and T_2-weighted MRI. In 19 (76%) of 25 patients with residual tumor, IMT uptake was located outside the T_2-weighted MRI changes. All 19 patients had high-grade gliomas. The pathologic IMT uptake areas were located up to 20 mm outside the hyperintensity on T_2-weighted MRI. Also, contrast enhancement and edema extended outside the area of IMT uptake, a consequence of postoperative BBB disturbances and edema. Because IMT-SPECT can visualize tumor tissue with a greater specificity and sensitivity than morphologic imaging modalities, we concluded that these findings could significantly modify target volumes for treatment planning and that the integration of amino acids tracers in treatment planning could help focus the high radiation dose on viable tumor tissue and protect normal brain tissue (Table 7).

MET-PET has a greater resolution (about 3–4 mm) than IMT-SPECT (about 7 mm); thus, MET-PET is more appropriate for use with high-precision radiation techniques (32). In our department, MET-PET is used in the treatment planning of patients with brain gliomas in two situations:

First, MET-PET has been integrated into a dose-escalation protocol for patients with residual tumor after surgery of high-grade gliomas. The GTV encompasses the region of MET uptake on the PET/MRI/CT fusion images. The CTV includes the GTV and the resection cavity plus a 2-cm margin, and the PTV1 is enlarged 0.5 cm to the CTV. The
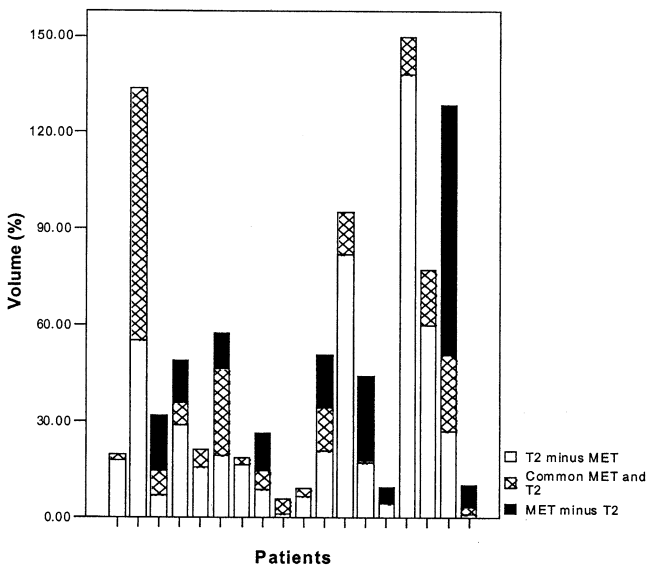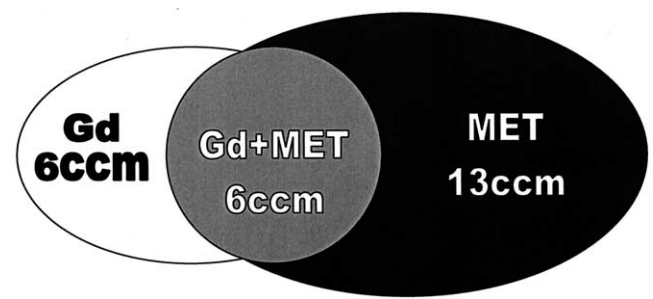

Fig. 6. T_2-weighted magnetic resonance imaging vs. L-(methyl-11C)-labeled methionine-positron emission tomography (MET-PET). Volumetric measurements using PET/MRI fusion for 18 patients with resected gliomas. White bars indicate hyperintensity outside of MET uptake; gray bars, both hyperintensity and MET uptake; and black bars, MET uptake without hyperintensity.

Table 5. Results of volumetric measurements in 18 patients with resected brain gliomas

Volume (cm^3)	T$_2$-weighted MRI	MET	Composite T2 and MET	Common T2 and MET	T$_2$-MET (minus)	MET-T$_2$ (minus)
Mean	42	23	52	13	29	10
Median	20	15	38	6	17	2
SD	44	27	46	18	35	19
Minimum	3	2	6	0	1	0
Maximum	150	102	150	78	138	78

MRI and MET-PET were performed 1–4 weeks postoperatively; volumetric measurements performed on PET/MRI fusion images; following volumes were quantified: volume of hyperintensity regions on T$_2$-weighted MRI, volume of MET uptake on PET, composite volume (Gd ∪ hyperintensity on T$_2$), common volume (Gd ∩ hyperintensity on T2), volume of hyperintensity on T$_2$ without (minus) MET uptake, and volume of MET uptake without (minus) corresponding hyperintensity areas on T$_2$-weighted MRI.

PTV1 is radiated to a total dose of 60 Gy (2 Gy/d, five times weekly) using a conventional three-dimensional technique. The dose is escalated on the macroscopic tumor volume using a stereotactic technique, with head fixation in a stereotactic mask. The PTV2 is defined as the MET uptake on the PET/MRI/CT fusion images (GTV) plus 3 mm. The dose delivered to the PTV2 is 20 Gy in 5 Gy/fraction four times weekly.

Second, MET-PET/CT/MRI fusion images are used in the treatment planning for repeat irradiation of recurrent high-grade gliomas. In such cases, we deliver a total dose of 30 Gy in 5 Gy/fraction, five fractions weekly, using a stereotactic technique. The GTV encompasses the MET on PET/MRI/CT fusion images. The GTV is not expanded to create the CTV. The PTV includes the GTV plus 3 mm.

One problem in the diagnosis of residual tumor using MET-PET could be the differentiation between tumor and granulation tissue after surgery. An increased amino acid transport into the cells is also described for macrophages, which are activated after surgery. However, several studies have demonstrated that this transport is significantly greater in tumor tissue than in inflammatory tissue (29). This differentiation is difficult to determine, especially for areas containing a small density of tumor cells. Therefore, we emphasize that MET-PET helps to delineate the regions with a high density of tumor cells, namely the macroscopic tumor tissue and not the microscopic tumor infiltration. In addition, histologic validation of the residual tumor regions on MET-PET is difficult because stereotactic biopsies in these regions would be another invasive approach in patients confronted with a bad prognosis and complex treatment. Therefore, the best noninvasive methods for valida-

tion of the clinical affect of MET-PET are clinical studies that investigate tumor control, recurrence location, and survival. The prognostic value of IMT-SPECT in patients with brain gliomas was analyzed in a previous study from our institution (40). The results of that study have indicated that in operated patients with gliomas, residual focal IMT is an important prognostic factor after tumor resection. For example, an IMT uptake ratio of >1.7 was associated with a fourfold greater risk of death. IMT uptake remained significantly correlated with survival when the important prognostic factors of age and tumor grade were included in a multivariate analysis. These findings strongly suggest that postoperative IMT uptake is a specific marker for residual tumor tissue and not an nonspecific sign reflecting reparative changes.

An important disadvantage of 11C-MET is the low physical half-time of about 20 min. The investigation necessitates an onsite cyclotron; therefore, the application of MET-PET has been mainly limited to academic research centers. The advantage of the amino acid analog, O-(2-[18F]Fluoro-ethyl)-L-Tyrosine (FET), is that it can be radiolabeled with fluorine-18, an isotope with a physical half-time of about 110 min and can be distributed to PET centers without an onsite cyclotron (41). In a preliminary analysis of 16 patients with brain gliomas, we found that MET-PET and FET-PET were equal in their ability to diagnose vital glioma tumor tissue (42). However, future clinical trials are required to confirm these results.

Table 6. Results of hyperintensity and MET comparison in 18 patients using PET/MRI fusion images

Finding	n (%)
MET uptake corresponded to hyperintensity on T$_2$	0/18 (0)
MET uptake located outside hyperintensity on T$_2$	9/18 (50)
Hyperintensity on T$_2$ located outside MET uptake	18/18 (100)

Areas with MET uptake on PET were compared, scan by scan, with the hyperintensity areas on T$_2$-weighted MRI.

MRI and MRS

Magnetic resonance imaging has been established as the best tool for visualizing brain and tumor anatomy, is of great importance when describing the tumor location and critical structures, and is very sensitive in detecting edema and BBB disruption. Therefore, MRI will remain the basis for diagnosis and treatment planning in patients with gliomas (13–15). However, when using MRI alone in resected patients, residual tumor cannot be differentiated from nonspecific postoperative changes, known to occur after the first 2 postoperative days. In addition, these changes can persist for months after surgery. Performing MRI in the first 2 postoperative days may increase the likelihood of detecting

Table 7. Comparison between mean volumes quantified on MET-PET/MRI fusion images in this study and mean volumes quantified on IMT-SPECT/MRI fusion images in previous study (35)

Vol-Gd (cm^3)	Vol-MET/IMT*	Composite Vol Gd and MET/IMT*	Common Vol Gd and MET/IMT*	Vol Gd-MET/IMT* (minus)	Vol MET/IMT-Gd* (minus)
11	19	24	6	6	13
12*	18*	27*	3*	9*	15*

Vol-T$_2$	Vol-MET/IMT*	Composite Vol T$_2$ and MET/IMT*	Common Vol T$_2$ and MET/IMT*	Vol T$_2$-MET/IMT* (minus)	Vol MET/IMT-T$_2$* (minus)
42	23	52	13	29	10
74*	18*	80*	12*	62*	6*

See text for description of terms.

Data presented as mean volume in cubic centimeters; second* and fourth* rows represent data determined using IMT (previous study [35]).Results of SPECT study showed mean volumes, computed in 25 operated patients with gliomas, for which IMT-SPECT detected residual tumor tissue after surgery.

"real" residual tumor. In this study we included patients with suspected residual tumor in the surgery report and/or on the MRI scans performed 24 hours postoperatively. In accordance, MET-PET showed residual tumor tissue in all investigated cases. It is generally not possible to use postoperative MRI, performed up to 2 days postoperatively, in treatment planning for the following reasons: (*1*) patients are acquired from different hospitals and as a consequence the technique of MRI is quite variable (e.g., Gd application, sequences used); (*2*) the MRI data sets from other departments cannot be coregistered with MET-PET; (*3*) MRI and MET-PET for treatment planning must be performed in the same week, before starting RT; and (*4*) an actual treatment planning MRI scan is usually performed about 3–4 days before beginning RT (i.e., 1–4 weeks postoperatively). During that interval, the regrowth of residual tumor cannot be excluded; thus, an actual reevaluation of tumor extension, using MET-PET, is always necessary. Therefore, we focused our trial on the comparison of MET-PET and MRI performed 2–3 weeks after surgery, for three-dimensional planning of RT.

T$_1$- and T$_2$-weighted images were analyzed because these sequences have been shown to correlate in several studies with the histologic findings and also because they are standard sequences used in treatment planning (43, 44). More sophisticated techniques, such as MRS, have also shown signs extending outside the T$_1$- and T$_2$-weighted MRI-derived target volume. In a previous study, Pirzkall *et al.* (45) used MRS and MRI in patients with malignant gliomas before and after surgery. They documented that metabolically active tumor cells existed up to 28 mm outside the T$_2$-weighted areas in as many as 88% of their preoperative patients. In a second study after surgery and before RT (46), MRS was also shown to be a valuable tool in the assessment of residual disease postoperatively. Both of these studies carry an important implication for the purpose of treatment planning in both resected and biopsy-only patients with malignant gliomas. These results are similar to our data,

even though another imaging tool was used for the investigation of brain gliomas.

CONCLUSIONS

Tumor imaging on MET-PET is based on the trait of tumor cells to transport the radiolabeled amino acids into the cell. This biologic feature is used for the visualization of tumor tissue. Therefore, based on a biologic paradigm, we defined a biologic target volume (19–21). In this case, the biologic target volume using MET-PET helped to describe the tumor morphology (GTV) with greater accuracy than using the traditional radiologic investigations (MRI or CT) alone. The biologic target volume (MET-PET) gives limited information about the malignancy of the tumor tissue. Data have shown that the intensity of amino acid uptake correlates with the grade of malignancy (47), but it is also known that low-grade gliomas, such as oligodendrogliomas, can have high amino acid transport (29). Thus, amino acids are useful in the description of the morphology, but not in the visualization of special biologic features of the tumor that describe the grade of malignancy. For this aspect, other tracers, such as markers for tumor proliferation, tumor hypoxia, or tumor angiogenesis need to be investigated.

The results of this study have shown that tumor volumes defined by MRI and MET-PET differ substantially. Because of the known high accuracy of MET-PET for the detection of tumor tissue, these findings suggest that MET-PET may significantly improve the definition of target volumes in patients with high-grade gliomas. MRI shows the contrast enhancement and edema, two features of the tissue related not only to tumor infiltration but also to postoperative changes. Using MET-PET/MRI fusion imaging, the biologic characterization of the tissue can be combined with an accurate presentation of the anatomy. This is a better tool for a precise delineation of the target volume, an essential step in the planning of RT.

REFERENCES

1. Deutch M, Green SB, Strike TA, *et al.* Results of randomized trial comparing BCNU plus radiotherapy, streptozocin plus radiotherapy, BCNU plus hyperfractionated radiotherapy, and BCNU following misonidasole plus radiotherapy in the postoperative treatment of malignant glioma. *Int J Radiat Oncol Biol Phys* 1989;16:1389–1396.

2. Kristiansen K, Hagen S, Kollevold T, *et al.* Combined modality therapy of operated astrocytomas grade III and IV: Confirmation of the value of postoperative irradiation and lack of potentiation of bleomycin on survival time—A prospective multicenter trial of the Scandinavian Glioblastoma Study group. *Cancer* 1981;47:649–652.

3. Nelson DF, Diener-West M, Weinstein AS, *et al.* A randomized comparison of misonidasole sensitized radiotherapy plus BCNU and radiotherapy plus BCNU for treatment of malignant glioma after surgery: Final report of an RTOG study. *Int J Radiat Oncol Biol Phys* 1986;12:1793–1800.

4. Chang CH, Horton J, Schoenfeld D, *et al.* Comparison of postoperative radiotherapy and combined postoperative radiotherapy and chemotherapy in the multidisciplinary management of malignant gliomas. *Cancer* 1983;52:997–1007.

5. Green SB, Byar DP, Walker MD. Comparison of carmustine, procarbazine, and high-dose methylprednisolone as additions to surgery and radiotherapy for the treatment of malignant glioma. *Cancer Treat Rep* 1983;67:121–132.

6. Levin VA, Silver P, Hannigan J, *et al.* Superiority of post-radiotherapy adjuvant chemotherapy with CCNU, procarbazine and vincristine (PCV) over BCNU for anaplastic astrocytoma: NCOG 6G91 final report. *Int J Radiat Oncol Biol Phys* 1990;18:321–324.

7. Jeremic B, Jovanovic D, Djuric L, *et al.* Advantage of post-radiotherapy chemotherapy with CCNU, procarbazine, and vincristine (mPCV) over chemotherapy with VM-26 and CCNU for malignant gliomas. *J Chemother* 1992;4:123–126.

8. Sneed PK, Gutin PH, Larson DA, *et al.* Patterns of recurrence of glioblastoma multiforme after external irradiation followed by implant boost. *Int J Radiat Oncol Biol Phys* 1994;29:719–727.

9. Mehta MP, Masciopinto J, Rozental J, *et al.* Stereotactic radiosurgery for glioblastoma multiforme: Report of a prospective study evaluating prognostic factors and analyzing long-term survival advantage. *Int J Radiat Oncol Biol Phys* 1994;30:541–549.

10. Schrieve DC, Alexander E III, Black PM, *et al.* Treatment of patients with primary glioblastoma multiforme with standard postoperative radiotherapy and radiosurgical boost: Prognostic factors and long-term outcome. *J Neurosurg* 1999;90:72–77.

11. Nelson DF, Diener-West M, Horton J, *et al.* Combined modality approach to treatment of malignant gliomas: Reevaluation of RTOG 7401/ECOG 1374 with long-term follow up—A joint RTOG-ECOG study. *Natl Cancer Inst Monogr* 1988;6:279–284.

12. Shapiro WR, Green SB, Burger PC, *et al.* Randomized trial of three chemotherapy regimens and two radiotherapy regimens in postoperative treatment of malignant glioma. *J Neurosurg* 1989;71:1–9.

13. Byrne TN. Imaging of gliomas. *Semin Oncol* 1994;21:162–171.

14. Sartor K. MR imaging of the brain tumors. *Eur Radiol* 1999; 9:1047–1054.

15. Galanis E, Buckner JC, Novotny P, *et al.* Efficacy of neuro-radiological imaging, neurological examination, and symptoms status in follow-up assessment of patients with high grade gliomas. *J Neurosurg* 2000;93:201–207.

16. Kelly PJ, Daumas-Duport C, Kispert DB. Imaged-based ste-reotaxic serial biopsies in untreated intracranial glial neoplasm. *J Neurosurg* 1987;66:865–874.

17. Kelly PJ, Daumas-Duport C, Scheitauer BW. Stereotactic histologic correlations of CT- and MRI-defined abnormalities in patients with glial neoplasms. *Mayo Clin Proc* 1987;62: 450–459.

18. Chamberlain MC, Murovic JA, Levin VA. Absence of contrast enhancement on CT brain scans of patients with supratentorial malignant gliomas. *Neurology* 1988;38:1371–13744.

19. Ling CC, Humm J, Larson S, *et al.* Towards multidimensional radiotherapy (MD-CRT): Biological imaging and biological conformality. *Int J Radiat Oncol Biol Phys* 2000;47:551–560.

20. Chapman JD, Bradley JD, Eary JF, *et al.* Molecular (functional) imaging for radiotherapy applications: An RTOG symposium. *Int J Radiat Oncol Biol Phys* 2003;55:294–301.

21. Grosu AL, Weber WA, Franz M, *et al.* Re-irradiation of recurrent high grade gliomas using amino-acids-PET (SPECT)/CT/MRI image fusion to determine gross tumor volume for stereotactic fractionated radiotherapy. *Int J Radiat Oncol Biol Phys* 2005; in press.

22. Ogawa T, Shishido F, Kanno I, *et al.* Cerebral glioma: Evaluation with methionine PET. *Radiology* 1993;186:45–53.

23. Lilja A, Bergström K, Hartvig P, *et al.* Dynamic study of supratentorial gliomas with L-methyl-11C-methionine and positron emission tomography. *Am J Neuroradiol* 1985;6: 505–514.

24. Hatazawa J, Ishiwata K, Itoh M, *et al.* Quantitative evaluation of L-[methyl-C-11] methionine uptake in tumor using positron emission tomography. *J Nucl Med* 1989;30:1809–1813.

25. Bergstrom M, Collins VP, Ehrin E, *et al.* Discrepancies in brain tumor extent as shown by computed tomography and positron emission tomography using [68Ga]EDTA, [11C]glucose, and [11C]methionine. *J Comput Assist Tomogr* 1983;7: 1062–1066.

26. Mosskin M EK, Hindmarsh T, Holst H, *et al.* Positron emission tomography compared with magnetic resonance imaging and computed tomography in supratentorial gliomas using multiple stereotactic biopsies as reference. *Acta Radiol* 1989; 30:225–232.

27. Ogawa T, Shishido F, Kanno I, *et al.* Cerebral glioma: Evaluation with methionine PET. *Radiology* 1993;186:45–53.

28. Braun V, Dempf S, Weller R, *et al.* Cranial neuronavigation with direct integration of (11)C methionine positron emission tomography (PET) data—Results of a pilot study in 32 surgical cases. *Acta Neurochir (Wien)* 2002;144:777–782.

29. Herholz K, Holzer T, Bauer B, *et al.* 11C-methionine PET for differential diagnosis of low-grade gliomas. *Neurology* 1998; 50:1316–1322.

30. Wienhard K, Dahlbom M, Eriksson L, *et al.* The ECAT EXACT HR: Performance of a new high resolution positron scanner. *J Comp Assist Tomogr* 1994;18:110–118.

31. Del Fiore G, Schmitz F, Plenevaux A, *et al.* Fast routine production of L-(11C-methyl)methionine with A1203/KF in a disposable unit. *J Labelled Cpd Radiopharm* 1995;37:746–748.

32. Grosu AL, Lachner R, Wiedenmann N, *et al.* Validation of a method for automatic image fusion (BrainLAB System) of CT data and 11C-methionine-PET data for stereotactic radiotherapy using a LINAC: First clinical experience. *Int J Radiat Oncol Biol Phys* 2003;56:1450–1463.

33. Berger MS. Malignant astrocytomas: Surgical aspects. *Semin Oncol* 1994;21:172–185.

34. Curran WJ Jr, Scott CB, Horton J, *et al.* Recursive partitioning analysis of prognostic factors in three Radiation Therapy Oncology Group malignant glioma trials. *J Natl Cancer Inst* 1993;85:704–710.

35. Ciric I, Ammirati M, Vick N, *et al.* Supratentorial gliomas: Surgical considerations and immediate postoperative results—Gross total resection versus partial resection. *Neurosurgery* 1987;21:21–26.

36. Langen HJ, Clauss RP, Holschbach M, *et al.* Comparison of iodotyrosines and methionine uptake in a rat glioma model. *J Nucl Med* 1998;39:1596–1599.

37. Langen KJ, Ziemons K, Kiwit JC, *et al.* 3-(123-I)iodo-alpha-methyltyrosine and (methyl-11C)-L-methionine uptake in cerebral gliomas: A comparative study using SPECT and PET. *J Nucl Med* 1997;38:517–522.

38. Grosu AL, Weber W, Feldmann HJ, *et al.* First experience with I-123-alpha-methyl-tyrosine SPECT in the 3-D radiation treatment planning of brain gliomas. *Int J Radiat Oncol Biol Phys* 2000;47:517–526.

39. Grosu AL, Feldmann H, Dick S, *et al.* Implications of IMT-SPECT for postoperative radiotherapy planning in patients with gliomas. *Int J Radiat Oncol Biol Phys* 2002;54:842–854.

40. Weber WA, Dick S, Reidl G, *et al.* Correlation between postoperative 3-(^{123}I)iodo-L-alpha-methyltyrosine uptake and survival in patients with gliomas. *J Nucl Med* 2001;42:1144–1150.

41. Wester HJ, Herz M, Weber WA, *et al.* Synthesis and radio-pharmacology of O-(2-[18F]fluoroethyl)-L-tyrosine for tumor imaging. *J Nucl Med* 1999;40:205–212.

42. Weber WA, Wester HJ, Grosu AL, *et al.* O-(2-[18F]fluoroethyl)-L-tyrosine and L-[methyl-11C]methionine uptake in brain tumors: Initial results of a comparative study. *Eur J Nucl Med* 2000;27:542–549.

43. Thornton AF, Sandler HM, Ten Haken RK, *et al.* The clinical utility of magnetic resonance imaging in 3-dimensional treatment planning of brain neoplasms. *Int Radiat Oncol Biol Phys* 1992;24:767–775.

44. Grosu AL, Feldmann HJ, Albrecht C, *et al.* Three-dimensional treatment planning of brain tumors: Advantages of the method and clinical results. *Strahlenther Onkol* 1998;174:7–13.

45. Pirzkall A, McKnight TR, Graves EE, *et al.* MR-spectroscopy guided target delineation for high-grade gliomas. *Int Radiat Oncol Biol Phys* 2001;50:915–928.

46. Pirzkall A, Li X, Joonmi O, *et al.* 3D MRSI for resected high-grade gliomas before RT: Tumor extent according to metabolic activity in relation to MRI. *Int Radiat Oncol Biol Phys* 2004;59:126–137.

47. Kaschten B, Stevenaert A, Sadzot B, *et al.* Preoperative evaluation of 54 gliomas by PET with fluorine-18-fluorodeoxyglucose and/or carbon-11-methionine. *J Nucl Med* 1998;39:778–785.